Advances in electromagnetic modeling based on integral equation methods and their application to 3D inversion of time-domain airborne data

Michael S. Zhdanov, The University of Utah and TechnoImaging, Leif H. Cox, Montana Tech and TechnoImaging, and Glenn A. Wilson, TechnoImaging*

Summary

Thirty-five years ago, Gerald W. Hohmann, late Professor of Geophysics at The University of Utah, published a seminal paper on 3D electromagnetic (EM) modeling using the integral equation (IE) method. This achievement subsequently inspired a considerable body of research in 3D EM modeling and inversion. Over the decades, the IE method evolved from the academic intrigue of EM fields scattering from simple 3D bodies into a practical tool of EM modeling and inversion for arbitrarily complex 3D geoelectrical structures. In this paper, we demonstrate that recent advances in the IE method have made it practical to rigorously invert entire surveys of time-domain airborne electromagnetic (AEM) data to 3D conductivity models with hundreds of thousands of cells within several hours on a workstation

Introduction

The integral equation (IE) method is a powerful method in 3D EM modeling and inversion for geophysical applications. It was originally introduced by Dmitriev (1969) in a paper which was published in Russian and along with the work of Tabarovsky (1975), long remained unknown to Western geophysicists. More than 35 years ago, Raiche (1974), Weidelt (1975) and Hohmann (1975) practically simultaneously published their famous papers on the IE method. Since then, generations of researchers have contributed to the development of the IE method (e.g., Wannamaker, 1991; Dmitriev and Nesmeyanova, 1992; Xiong, 1992; Xiong and Kirsch, 1992; Avdeev et al., 2002; Hursán and Zhdanov, 2002; Zhdanov, 2002; Singer et al., 2003; Abubakar and van der Berg, 2004; Avdeev, 2005). The main advantage of the IE method when compared to finite-difference (FD) or finite-element (FE) methods is the fast and accurate simulation of EM data for models of compact 3D targets embedded in layered backgrounds. Traditional implementations of the IE method result in small but full linear systems that can be solved using direct methods. However, the governing equations of the IE method can also be considered as convolutions of the Green's tensors and scattered currents, meaning the linear system can be decomposed to Toeplitz or block-Toeplitz structures. For iterative solvers, this means 2D FFT convolutions can be used for fast matrix-vector multiplications, resulting in a significant decrease in runtimes compared conventional implementations of iterative solvers (Hursán and Zhdanov, 2002).

FD and FE methods are required to discretize the entire model domain, encompassing not only the targets of interest, but a larger volume about them and often including the air which results in large but sparse linear systems. While IE methods avoid this, it is recognized (even emphasized as early as Dmitriev, 1969) that the main limitation of the IE method is that the background conductivity model must have a 1D structure to allow for semi-analytic forms of the Green's functions. Any deviation from the background model must be treated as an anomalous conductivity. In many practical applications however, it is difficult to describe a model using horizontally layered background conductivity. In such cases, the model domain can become too large for the available computer memory and/or computational time. It was demonstrated by Zhdanov et al. (2006) that one can overcome this difficulty by using models with inhomogeneous background conductivity (IBC). This approach is very practical when modeling geological features such as topography, inhomogeneous overburden, or salt dome structures. This situation occurs, for example, when we have known information about the existence of specific geoelectrical structures which should be considered in modeling and/or inversion.

There are several advantages to the IE method for 3D inversion compared to more traditional FD or FE approaches. First, forward modeling with the IE method requires the calculation of the Green's tensors for the background conductivity model. These Green's tensors can be precomputed and saved for use in the many iterations of inversion; a saving which significantly speeds up the computation of the predicted data on each iteration. Second, those same precomputed Green's tensors can be readily used for Fréchet derivative calculations, which is another important element of inversion. Finally, IE forward modeling and inversion requires the discretization of the inversion domain only, while in FD or FE methods, one has to discretize the entire model domain. Moreover, in cases of controlled-source or airborne EM methods, one can exploit the fact that the area of the footprint of a transmitter-receiver pair is significantly smaller than the area of the EM survey to develop a robust 3D inversion method which uses a moving system footprint approach. In this paper we demonstrate the effectiveness of such an IE approach to 3D inversion with a case study for time-domain airborne electromagnetic (AEM) data.

Advances in electromagnetic modeling and inversion based on integral equation method

Time-domain airborne electromagnetic (AEM) data

Currently, the interpretation of AEM data is based on direct transformation of the data into 1D conductivity-depth images (CDI/CDT) or by layered earth inversions. The large-scale 3D inversion of entire AEM datasets is perceived as intractable, even with access to high performance computing resources. Thus it is common practice to rely on various 1D methods for time-domain AEM interpretation. Difficulties with 3D interpretation of AEM data stem from the fact that the forward modeling and sensitivities calculations, required for inversion, should be repeated for multiple transmitter positions and iterations.

While in theory the sensitivity matrix for an AEM survey is full, in practice it is effectively sparse due to the relatively limited footprint of the AEM system. As an example for frequency-domain AEM systems, Liu and Becker (1990) determined at the inductive limit, the footprints for the horizontal coplanar and vertical coaxial components are 3.75h and 1.35h, respectively, where h is the flight height of the transmitter. Reid et al. (2006) showed that the footprints may be as large as 10 times the flight height for low induction numbers, meaning that the footprint maybe less than 400 m for frequency-domain AEM systems. Regardless, the area of the footprint is less than the area of the survey. In order to compute the fields and sensitivities for a given transmitter-receiver pair, one needs only to simulate a subset of the 3D conductivity model that encapsulates the AEM system's footprint (Figure 1). The sensitivity matrix for the 3D conductivity model can then constructed as the superposition of footprints for all transmitter-receiver pairs. This effectively spare storage of the sensitivity matrix significantly reduces memory requirements.

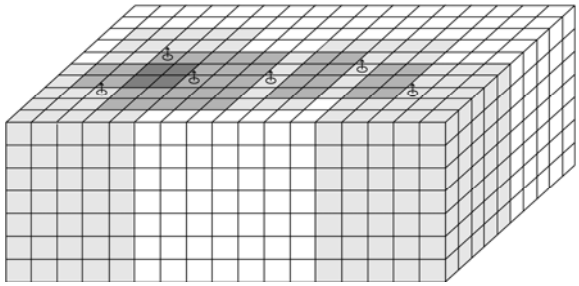

Figure 1. *Schematic diagram of different footprints (shaded) superimposed over the 3D conductivity model. Those cells in darker shading are where different footprints overlap.*

Using this moving footprint approach, we extend the work by Cox et al. (2010) to show that it is practical to invert entire time-domain AEM surveys and recover 3D conductivity models with hundreds of thousands of cells within a day on a workstation.

3D inversion of time-domain AEM data

Regularized inversion is based on minimization of the Tikhonov parametric functional, $P^{\alpha}(\boldsymbol{\sigma})$:

$$P^{\alpha}(\boldsymbol{\sigma}) = \phi(\boldsymbol{\sigma}) + \alpha s(\boldsymbol{\sigma}), \qquad (1)$$

where $\phi(\boldsymbol{\sigma})$ is a misfit functional between the observed and predicted data, $s(\boldsymbol{\sigma})$ is a stabilizing functional, and α is the regularization parameter that trades-off between the misfit and stabilizing functional. There are essentially two methods of minimizing equation (1). One approach is with a Gauss-Newton method which updates the vector of conductivities so as to minimize the vector of residual errors using the iterative scheme:

$$\boldsymbol{\sigma}_{i+1} = \boldsymbol{\sigma}_i + \Delta\boldsymbol{\sigma}_i = \boldsymbol{\sigma}_i + k_i \mathbf{F}_i^{+} \mathbf{r}_i, \qquad (2)$$

where k_i is a step length, $\mathbf{F}_i^{+}$ is the generalized inverse of the $N_d \times N_m$ Fréchet matrix $\mathbf{F}_i$ of normalized sensitivities, and $\mathbf{r}_i$ is the N_d length vector of the residual fields between the observed and predicted data on the i^{th} iteration. While the number of iterations is minimized since Gauss-Newton methods generally exhibit near-quadratic convergence, there is non-trivial expense in the computation of the generalized inverse of the Fréchet matrix at each iteration. For very large-scale inversions, this is actually impractical to compute. In such cases, an alternative, practical solution for solving equation (1) is with one of the steepest descent methods which iteratively update the vector of anomalous conductivities so as to minimize the vector of residual errors using the iterative scheme:

$$\boldsymbol{\sigma}_{i+1} = \boldsymbol{\sigma}_i + \Delta\boldsymbol{\sigma}_i = \boldsymbol{\sigma}_i + k_i \mathbf{F}_i^{*} \mathbf{r}_i, \qquad (3)$$

where k_i is a step length and $\mathbf{F}_i^{*}$ is the conjugate transpose of the Fréchet matrix. Convergence of the steepest descent method is improved by including conjugate gradient terms. We have implemented the reweighted regularized conjugate gradient method (Zhdanov, 2002, 2009), whereby data and model weights re-weighting the inverse problem in logarithmic space are introduced in order to reduce the dynamic range of both the data and conductivity. Sensitivities are computed using adjoint operators. The inversion iterates until the residual error reaches a pre-set threshold, the decrease in error between multiple iterations becomes less than a pre-set threshold, or a maximum number of iterations is reached.

In a moving footprint inversion, each transmitter-receiver pair is assumed to contain sensitivity to those cells within its footprint only, and not the entire 3D model. This is

equivalent to setting all irrelevant sensitivities to zero, and means we can exclude those cells outside the AEM's footprint by excluding them from the summation. Equation (3) is modified to, for example:

$$\Delta\sigma_{i,j} = k_i \sum F^*_{n,j} r_n, \quad (4)$$

where the *n* and *j* subscripts relate the indices of cells and data pertaining to each transmitter-receiver pair.

3D modeling of time-domain AEM data

3D AEM inversion requires fast and accurate modeling. The anomalous (*a*) electromagnetic fields are computed as an integral equation of the induced currents **J** in a 3D model domain *V* filled with anomalous conductivity superimposed on a background conductivity model:

$$\mathbf{E}^a(\mathbf{r}') = \iiint_V \widehat{\mathbf{G}}_E(\boldsymbol{r}', \boldsymbol{r}) \cdot \mathbf{J}(\mathbf{r}) dv, \quad (5)$$

$$\mathbf{H}^a(\mathbf{r}') = \iiint_V \widehat{\mathbf{G}}_H(\boldsymbol{r}', \boldsymbol{r}) \cdot \mathbf{J}(\mathbf{r}) dv. \quad (6)$$

The contraction integral equation method modifies the Green's operator to have a norm less than one, which effectively preconditions conventional implementations of the 3D integral equation method. However, the full scattering matrix poses the largest obstacle to solving integral equations (5) and (6), as its direct inversion with complexity $O(n^3)$ can be computationally prohibitive. While direct solvers may offer advantage for AEM modeling by simultaneously solving multiple right-hand side source vectors, they require anew decomposition for each 3D conductivity model. This makes them inefficient for moving footprint inversion. Iterative schemes reduce complexity to $O(n^2)$, however they must be solved anew for each right-hand side source vector. Integral equations (5) and (6) can be considered as convolutions of the Green's operators and the induced currents. When the 3D model domain is regularly discretized in the horizontal directions, the scattering matrix reduces to a Toeplitz structure; the exploitation of which results in fast matrix-vector multiplications as 2D FFT convolutions that reduce complexity from $O(n^2)$ to $O(n\log n)$ (Hursán and Zhdanov, 2002). For a moving footprint, the body-body Green's tensors are horizontally invariant, meaning they are identical for each footprint domain and thus can then translated over the entire inversion domain, speeding up the computation and increasing memory efficiency. Moreover, once the Green's tensors have been pre-computed, they are stored and re-used in subsequent iterations, further reducing runtime. The IBC IE method also allows us to consider those geoelectrical models with inhomogeneous background conductivity so as to introduce topography and/or regional geoelectrical structures into the inversion (Zhdanov et al., 2006). For time-domain AEM, the model responses and sensitivities are computed at 28 frequencies logarithmically spaced from 1 Hz to 100 kHz. These are splined and extrapolated back to zero frequency. These responses and sensitivities are Fourier transformed into several pulse lengths and then folded back into one, and differentiated if necessary, before being convolved with the transmitter waveform in the time-domain and integrated over the receiver windows (Raiche, 1998).

Model study

We demonstrate the effectiveness of our 3D inversion with a VTEM model study over a thin plate with 5 S/m conductance embedded at 50 m depth in an otherwise 500 Ωm homogeneous half-space. The synthetic data were computed using *LeroiAir* (Raiche et al., 2007). The VTEM system has a 50% duty cycle bipolar square wave form with base frequency of 25 Hz. The transmitter loop consists of 4 turns over an area of 531 m^2. 27 off-time channels of vertical data were simulated out to 16.74 ms. 891 stations were simulated at 25 m station spacing and 100 m line spacing over a flat plate with dimensions of 400 m x 400 m buried 50 m below the surface. Starting from a 500 Ωm homogeneous half-space model, the 3D conductivity model recovered from inversion is shown in Figure 2, as is the position of the plate.

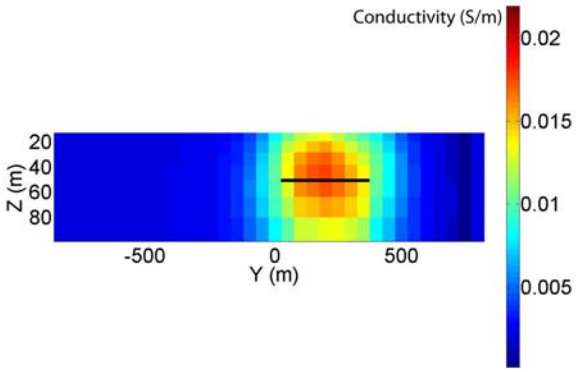

Figure 2. *Conductivity model recovered from 3D inversion of VTEM data over a flat plate (shown in black).*

Case study – Bookpurnong, South Australia

It is often argued that AEM interpretation for salinity mapping is ideally suited to the various 1D methods because of the high conductance of the ground, relative continuity of horizons, and their ability to rapidly generate pseudo-3D conductivity models of entire surveys. Such an example is at the Bookpurnong Irrigation District located along the Murray River, approximately 12 km upstream from the township of Loxton, South Australia. This area

has been the focus of various geophysical trials to manage a decline in vegetation; largely in response to floodplain sanitization from groundwater discharge in combination with decreased flooding frequency, permanent weir pool levels and drought. Ground-based, river-borne and AEM methods have been deployed with the intent of mapping the distribution of salinity in the floodplain soils and groundwater. We refer the readers to Munday et al. (2007) for a more detailed description of the geology, hydrology, and various river, borehole, ground and airborne electromagnetic surveys.

The area was flown with the SkyTEM time-domain helicopter system in April 2007. The SkyTEM system was configured with both low and high moment modes. We concern ourselves only with the high moment data, which corresponds to a 50% duty cycle quarter sine wave with peak current of about 90 A, and base frequency of 25 Hz. 26 off-time channels of inline and vertical data were recorded out to 19.8 ms. The transmitter loop consists of 4 turns over an area of 314 m^2. This 162 line km survey was flown as 29 lines oriented in a NW-SE direction similar to the RESOLVE survey also flown in the area (Cox et al., 2010), with 100 m line spacing, and one tie line. Additional flight lines were acquired along the Murray River. The survey consisted of a total of 5510 stations, all of which were used in the 3D inversion. The survey was flown with a nominal bird height of approximately 60 m.

The SkyTEM data were inverted for a 3D conductivity model with approximately 210,000 cells that were 35 m x 35 m in the horizontal directions, and varied from 4.8 m to 33 m in the vertical direction. This grid was superimposed on a layered half-space with a 10m thick 10Ωm layer over a 1Ωm half-space. The footprint of the SkyTEM system was set at 280 m. The 3D inversion of the SkyTEM data required 10 hours on a Linux workstation with eight 2.4 GHz processors and 24 GB RAM. Figure 2 shows a slice of the model at 4 m depth derived from the 3D inversion of the SkyTEM data. The Murray River, which has a lower conductivity than the floodplains, is clearly visible in the 3D inversion results. At depth, the 3D inversion creates a coherent image of the losing and gaining sections of the Murray River.

Conclusions

Since a publication of Gerald W. Hohmann's seminal paper in 1975, the IE method has evolved from a purely theoretical technique for studying simple academic problems into a practical tool of 3D EM modeling and inversion. Today, the IE method can be used for solving large-scale 3D inverse problems where the geoelectrical models can be discretized into hundreds of thousands, even millions of cells. The advantage of the IE method is that it not only ensures a rigorous solution for the forward problem, but also provides an effective way for computing sensitivities and/or adjoint operators required in 3D EM inversion.

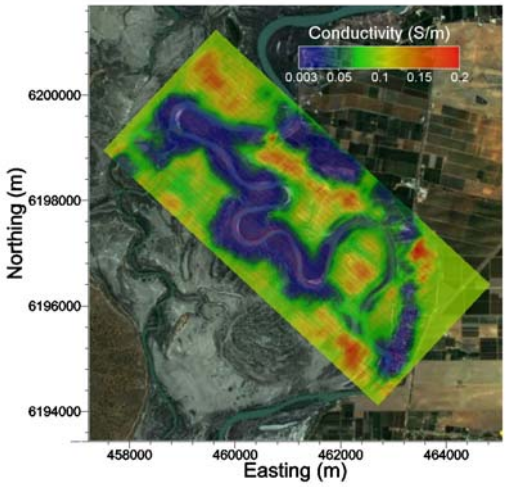

Figure 5. *Horizontal cross-section at 4 m depth of conductivity extracted from the 3D inversion of the SkyTEM data.*

It is often argued that 1D methods are the only practical approach to interpreting time-domain AEM data. As we have demonstrated with our case study, that is not the case. The IE method makes 3D inversion of entire time-domain AEM surveys a practical consideration, with runtimes of several hours on a serial workstation. We have achieved this by exploiting the fact that the area of a time-domain AEM system's footprint is much smaller than the area of a typical AEM survey and encapsulated that into our IE based 3D inversion methodology. Our implementation naturally lends itself to large-scale parallelization, and we are currently in the process of distributing our software on massively parallelized architectures. This will allow for a further decrease in the runtime, and will make it possible to invert even larger time-domain AEM surveys.

Acknowledgements

The Bookpurnong SkyTEM data presented in this paper were financed in part by the South Australian CNMR Board Project 054127: *The application of airborne geophysics to the prediction of groundwater recharge and floodplain salinity management*, and the CSIRO National Flagship program Water for a Healthy Country through the Regional Water theme. We also acknowledge TechnoImaging for support of this research, and Zhdanov acknowledges support from The University of Utah's Consortium for Electromagnetic Modeling and Inversion (CEMI).

References

Abubakar, A., and P. M. van der Berg, 2004, Iterative forward and inverse algorithms based on domain integral equations for three-dimensional electric and magnetic objects: J. Comp. Phys., **195,** 236-262.

Avdeev, D. B., 2005, Three-dimensional electromagnetic modeling and inversion from theory to application: Surv. Geophys., **26,** 767-799.

Cox, L. H., G. A. Wilson and M. S. Zhdanov, 2010, 3D AEM inversion with a moving footprint – a case study for salt mapping at Bookpurnong, South Australia: Presented at 23rd SAGEEP.

Dmitriev, V. I., 1969, Electromagnetic fields in inhomogeneous media (in Russian): Proc. Computational Center, Moscow State University.

Dmitriev, V. I., and N. I. Nesmeyanova, 1992, Integral equation method in three-dimensional problems of low-frequency electrodynamics (in Russian): Computational Mathematics and Modeling, **3,** 313-317.

Hohmann, G. W., 1975, Three-dimensional induced polarization and electromagnetic modeling: Geophysics, **40**, 309-324.

Hursán, G., and M. S., Zhdanov, 2002, Contraction integral equation method in three-dimensional electromagnetic modeling: Radio Sci., **37**, doi: 10.1029/2001RS002513.

Liu, G., and A. Becker, 1990, Two-dimensional mapping of sea-ice keels with airborne electromagnetic: Geophysics, **55**, 239-248.

Munday, T., A. Fitzpatrick, J. Reid, V. Berens, and D. Sattel, 2007, Frequency and/or time-domain HEM systems for defining floodplain processes linked to the salinisation along the Murray River: Presented at 19th ASEG Geophysical Conference and Exhibition.

Raiche, A. P., 1974, An integral equation approach to three-dimensional modeling: Geophys. J. R. astr. Soc., **36**, 363-376.

Raiche, A., 1998, Modelling the response of AEM systems: Explor. Geophys., **29**, 103-106.

Raiche, A., F. Sugeng, and G. Wilson, 2007, Practical 3D EM inversion – P223F software suite: Presented at 19th ASEG Geophysical Conference and Exhibition.

Reid, J. E., A. Pfaffling, and J. Vrbancich, 2006, Airborne electromagnetic footprints in 1D earths: Geophysics, **71**, G63-G72.

Singer, B. Sh., A. Mezzatesta, and T. Wang, 2003, Integral equation approach based on contraction operators and Krylov subspace optimisation, in Macnae, J., and G. Liu, Eds., Three-dimensional Electromagnetics III, Australian Society of Exploration Geophysicists.

Tabarovsky, L. A., 1975, Application of integral equation method to geoelectric problems (in Russian): Nauka.

Wannamaker, P. E., 1991, Advances in three-dimensional magnetotelluric modeling using integral equations: Geophysics, **56**, 1716-1728.

Weidelt, P., 1975, Electromagnetic induction in three-dimensional structures: J. Geophysics, **41**, 85-109.

Xiong, Z., 1992, Electromagnetic modeling of 3-D structures by the method of system iteration using integral equations: Geophysics, **57,** 1556-1561.

Xiong, Z., and A. Kirsch, 1992, Three-dimensional earth conductivity inversion: J. Comp. App. Math., **42,** 109-121.

Zhdanov, M. S., 2002, Geophysical Inverse Theory and Regularization Problems: Elsevier.

Zhdanov, M. S., 2009, Geophysical Electromagnetic Theory and Methods: Elsevier.

Zhdanov, M. S., S. K., Lee, and K. Yoshioka, 2006, Integral equation method for 3D modeling of electromagnetic fields in complex structures with inhomogeneous background conductivity: Geophysics, **71**, G333-G345.